

SUPERCRITICAL WATER (SCW): A NEW MEDIUM TO GENERATE NOVEL MATERIALS FOR SOLAR ENERGY APPLICATIONS

Janusz A. Kozinski*¹, Morgan L. Thomas¹, Ian S. Butler², Ajay K. Dalai³

¹Department of Earth and Space Science and Engineering, York University, Toronto, Canada

²Department of Chemistry, McGill University, Montreal, Quebec, Canada

³Department of Chemical and Biological Engineering, University of Saskatchewan, Saskatoon, Canada

*Corresponding author: janusz.kozinski@yorku.ca; Phone: (+1) 416 736-5484

ABSTRACT

We present here developments and results from a multidisciplinary experimental program focused on the use of supercritical water (SCW) for energy applications and hydrothermal processing. We highlight our findings from investigating the interaction of organic and inorganic materials with SCW, and also comment on progress with advanced measurement systems. Supercritical water (SCW) possesses unique properties, which have prompted investigation into its usage in a plethora of energy and chemical applications. Beyond its critical point (374 °C and 22.1 MPa), water exhibits unconventional solubility and heat transfer characteristics, which are potentially advantageous. In this paper, we present an overview of our progress in experimental studies of the interaction of SCW with a variety of materials, both organic and inorganic. Our most notable progress has been in the development of several novel materials, designs and experimental techniques for small-scale research, and the use of these designs and techniques for detailed experimental study. The work shown highlights the potential of SCW as a useful medium for solar energy applications, and identifies some intriguing features of SCW research.

INTRODUCTION

The study of hydrothermal systems for energy processes has been an active research area for many years, with there even being some limited examples of industrial application [1-3]. The results presented here represent an advancement of our efforts to develop the Hydrothermal Diamond Anvil Cell (HDAC) as a valuable experimental tool for *in situ* measurements under hydrothermal or supercritical water (SCW) conditions. Our particular interest is focused on the use of SCW as a reaction medium for materials conversion [4-10]. The potential for hydrothermal processing as a unique and efficient method for biomaterials conversion has previously been demonstrated for various other experimental setups [11-14]. We report here on our successful efforts to perform *in situ* synchrotron X-ray powder diffraction (XRPD) and laser micro-Raman spectrometry analyses of variety of cellulose-based materials under hydrothermal conditions using the HDAC.

We describe a new approach and discuss our results, which agree with established mechanisms for cellulose evolution, and allow us to propose, for the first time, a more detailed hypothesis for transformation within a supercritical water-dominated environment in terms of particulate behaviour. We also comment on the production of rare-earth metal compounds, particularly the pyrophosphate, $\text{ErKP}_2\text{O}_7 \cdot 2\text{H}_2\text{O}$, and the tricyclophosphate, $\text{ErNa}_3(\text{P}_3\text{O}_9)_2 \cdot 9\text{H}_2\text{O}$, as well as other erbium-based materials, which can be applied in solar energy systems.

EXPERIMENTAL

Selected experiments were performed using a Hydrothermal Diamond Anvil Cell (Foxwood Instruments, NY) [15]. The HDAC permits *in situ* measurements at high temperature and pressure, and has been described in detail elsewhere [16, 17]. All chemicals were purchased from Sigma-Aldrich and were used without further purification. A stainless-steel gasket, 250 μm in thickness, with sample chamber of 250 μm o.d., was used in all the experiments. The sample chamber was loaded with distilled water and analyte under a constant flow of nitrogen, which was maintained during the heating cycle of the cell.

Raman spectra were recorded on a Renishaw *inVia* Raman microscope system using either 514.5- or 785-nm laser excitation. Calibration of the Raman spectrometer was performed prior to each set of measurements with a standard Si wafer. The proprietary software Renishaw *WiRE*TM (version 3.2), was used for data acquisition and processing. Focussing was achieved with a super long-working distance 20x objective (Olympus SLMPLN20X).

X-ray powder diffraction was performed using the Hard X-ray Micro Analysis (HXMA, 06ID-1) beamline at the Canadian Light Source (Saskatoon, Saskatchewan), Canada's national synchrotron radiation facility. The cell was mounted on a motorized swivel stage (SA05B-RL, Kohzu Precision, Japan), allowing for angular rotation of the cell, which was itself mounted on a second stage to provide vertical and horizontal motion. The cell was fixed in position on the stage using an insulating U-shaped mount to prevent heat dissipation from the cell to sensitive components. A 250 μm pinhole was used to prevent interferences from beam divergence and scattering. The layout of the associated equipment in the experimental hutch has been described in detail earlier [18]. Shown in Fig. 1a

and 1b is an image and sketch of the setup used in our experiments.

X-ray diffraction images were recorded on a MAR345 image plate detector (Marresearch, Norderstedt, Germany) at the HXMA beamline. Exposure times were 60 s unless otherwise noted, with $\lambda = 0.509175 \text{ \AA}$. Calibration was performed using a NIST lanthanum hexaboride (LaB_6) standard. Baseline correction and final processing of the resultant powder patterns were performed with FullProf Suite (1.10) software.

Raman spectroscopic measurements at the beamline were conducted using a Renishaw RM 2000 Raman microscope system coupled to a Renishaw RP20 fiber optic probehead with 514.5-nm laser excitation. The probe head also incorporated a Philips ToUcam PRO II (1.2 Megapixel) CCD camera, which was used to obtain images of the sample in the HDAC. The probe was positioned parallel to the X-ray beam path and the HDAC was moved between the two positions as shown in Fig. 1a and 1b to measure images (position 1) and X-ray patterns (position 2).

DISCUSSION: HYDROTHERMAL STUDIES

We have previously reported on the decomposition of glucose, cellulose and lignocellulose under hydrothermal conditions [4, 20]. Our approach in the present work has been to extend the study with the use of more advanced analytical techniques. In the initial stage, we measured the micro-Raman spectra of microgranular cellulose in the HDAC. As this organic material is a rather weak Raman scatterer, ideally a prolonged measurement must be performed (e.g., 30 min) to achieve a reasonable signal-to-noise ratio. In this work, the approach taken to avoid long data acquisition time was to select small spectral windows in an attempt to identify chemical changes as they occurred. Having identified two key regions of interest (namely 300-500 and 900-1200 cm^{-1} , see Fig. 1), we proceeded with an investigation of the changes in the spectra with increasing temperature in the HDAC, as shown in Figure 1a. In the 900-1200 cm^{-1} region, we observed a clear loss of cellulose crystallinity at temperatures greater than 225 °C.

Our initial synchrotron experiments, using the set-up shown in Figs 1b and 1c, employed these Raman data as a basis for experimental validation. Further details of the experimental methods are provided in the supplementary information. Figure 2 shows an analogous experiment for measurement of X-ray diffraction of cellulose with increasing temperature in the HDAC. Again, we observed a clear loss of crystallinity at temperatures greater than 225 °C. Notably, the initial diffraction pattern (and indeed the initial Raman spectrum) was not recovered upon cooling of the sample, implying that the change is irreversible. This is in agreement with the mechanisms we proposed earlier for cellulose conversion under hydrothermal conditions, with an initial step of cellulose dissolution and depolymerisation (hydrolysis), followed by reaction of the component sugars [7-10, 21-23]. The significance of this measurement relates to defining a means to identify the point of loss of crystallinity, hence dissolution of the cellulosic components, and possible use in refining existing kinetic models for this transformation.

Our subsequent work has dealt with the measurement of XRPD data for other important solid materials that are present in biomass residue, measurement of pressure, and the ongoing development of the Raman system for simultaneous (same-spot) XRPD and micro-Raman measurements. A brief discussion on the limitation of the combined technique, in particular with regard to the reliable measurement of pressure under reaction conditions is provided in the supporting information.

We employed several different calcium-based compounds as models for the residue that may be produced from the hydrothermal decomposition reactions of lignocellulosic materials. These model compounds were selected based on earlier reports of their transformation under hydrothermal or high-pressure conditions, the prevalence of calcium-containing deposits from SCW biomass conversion [5] and the high proportion of calcium in certain woody species [24-26].

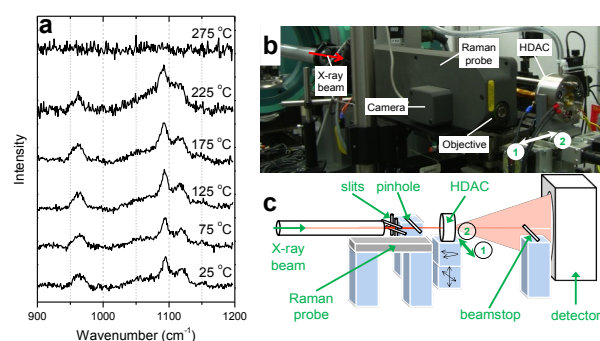


Figure 1: (a) Raman spectra (785 nm laser line) for cellulose with increasing temperature showing the loss of crystallinity at temperatures $>225 \text{ °C}$, (b) image and (c) sketch (not to scale) of synchrotron set-up for XRPD measurements in the HDAC at the HXMA beamline. The cell was shuttled between position 1 (Raman/camera) and position 2 (X-ray) for these measurements.

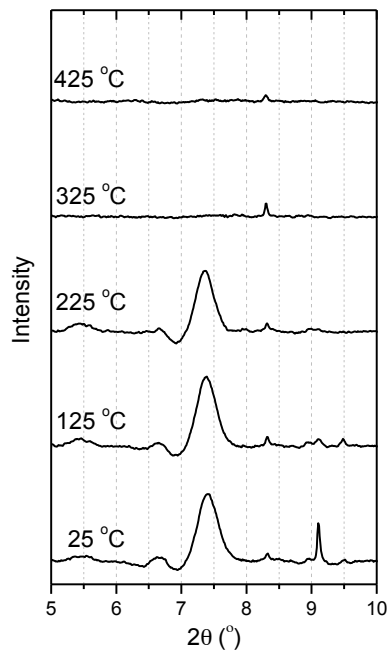


Figure 2: XRPD patterns for cellulose with increasing temperature showing the loss of crystallinity at temperatures $>225\text{ }^{\circ}\text{C}$

Calcium oxalate is a species known to be present in a wide variety of types of biomass and plays a key role in structural and biochemical processes. In some cases, it is present in crystalline form in plant tissues. Figure 3 shows the visible changes occurring in the cell during the heating experiment. With a suitable choice of heating rate, it was possible to collect the images at position 1 (see Fig. 1b and c regarding the location of position 1 and 2), move the cell while heating to position 2, perform the XRPD measurement and finally return the cell to position 1 while reading the detector image plate. Thus, the data collection can be performed in a relatively short time period (i.e., 45-60 min).

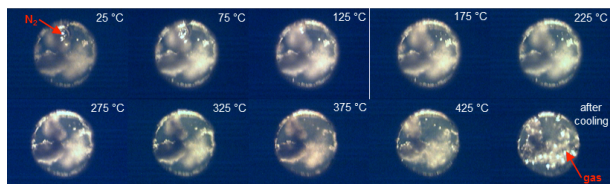


Figure 3: Images of calcium oxalate in HDAC with increasing temperature showing qualitatively the change in the material during heating, and the N_2 bubble dissolution used for pressure determination ($T_h = 150\text{ }^{\circ}\text{C}$, $\rho = 917.01\text{ kg/m}^3$).

The XRPD data measurements performed for calcium oxalate under hydrothermal conditions show a dramatic change in the powder pattern at a temperature close to the critical temperature of pure water ($T_c = 374\text{ }^{\circ}\text{C}$), as shown in Fig. 4. Similar to the earlier observations with cellulose, the crystalline component of the sample appears to react and is not present in the pattern obtained after cooling. Moreover, there was an increased amount of gaseous products present in the sample volume after cooling (see Fig. 5). We suggest that calcium oxalate under these conditions reacts irreversibly via a decarboxylation or decarbonylation pathway, producing CO_2 or CO , respectively.

Calcium hydroxyapatite and related materials are known to undergo structural transformations at hydrothermal conditions and at high pressures [27, 28]. In our XRPD study of this material, however, we observed no significant changes with increasing temperature, as shown in Fig. 5. It should be emphasized that our study was principally concerned with the understanding of rapid processes for application in chemical reactors, whereas the structural changes reported in the literature are most likely due to less rapid transformations. The stability of this material under the tested conditions provides an indication of the types of material that may be present in the residue following prolonged hydrothermal treatment.

DISCUSSION: NOVEL MATERIALS STUDIES

Our research has had an emphasis on the production of rare-earth metal compounds, particularly the pyrophosphate, $\text{ErKP}_2\text{O}_7 \cdot 2\text{H}_2\text{O}$, and the tricyclophosphate, $\text{ErNa}_3(\text{P}_3\text{O}_9)_2 \cdot 9\text{H}_2\text{O}$, as well as other erbium-based materials,

which can be applied in solar energy systems. In the structure of the pyrophosphate salt, one-dimensional heptagonal channels are formed along the slightly inclined a-axis with the following dimensions: $5.6 \times 6.7\text{ \AA}$, while that of the tricyclophosphate consists of alternating layers of $[\text{P}_3\text{O}_9]^{3-}$ groups, ErO_8 dodecahedra, $\text{Na}(1)\text{O}_6$ and $\text{Na}(2)\text{O}_7$ polyhedra linked together by water molecules.

The P_3O_9 rings in this latter compound are grouped together along the c-axis in a $\text{P}_3\text{O}_9\text{-ErO}_8$ arrangement thereby producing broad, hexagonal channels of diameter of 6.65 \AA with a side dimension of 3.907 \AA . Spectra of $\text{ErKP}_2\text{O}_7 \cdot 2\text{H}_2\text{O}$ have been measured and interpreted. We also developed a simple hydrothermal synthetic approach to produce a number of new erbium-based materials in the form of crystalline microflowers, hexagonal microlayers, microsticks and microspheres, which are comprised of nanoparticles, as well as nanofibers, nanorods and nanolayers. Their crystallinity, morphology, optical properties and structural features have been examined and potential applications in solar energy systems considered.

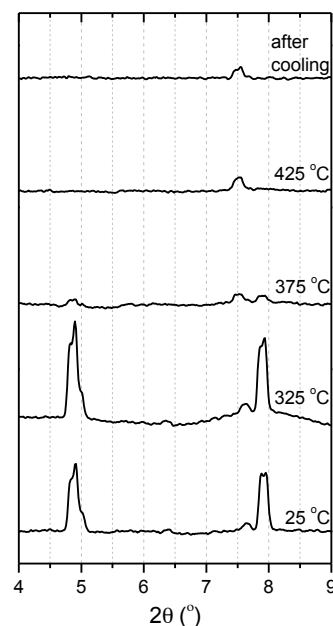


Figure 4: XRPD patterns for calcium oxalate with increasing temperature showing the change in structure at around $375\text{ }^{\circ}\text{C}$ (patterns between 25 and $325\text{ }^{\circ}\text{C}$ omitted for clarity).

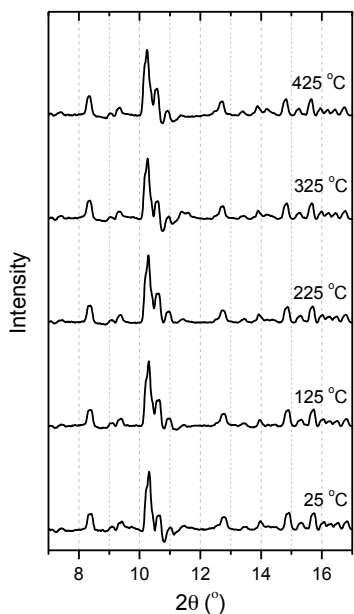


Figure 5: XRPD patterns for hydroxyapatite with increasing temperature ($T_h = 225\text{ }^\circ\text{C}$, $\rho = 833.75\text{ kg/m}^3$) showing little change over the studied range

CONCLUSIONS

Supercritical water remains a promising alternative to conventional chemical and materials processing technologies. We have demonstrated in this work some key analyses to aid in our understanding of the fundamental processes that occur during the hydrothermal transformations of biomaterials models. Our results provide new insights into the chemical pathways involved in the production of solid residues. We have also demonstrated the usefulness of synchrotron science for SCW conversion research. Specifically, the use of XRPD as an in situ measurement tool is invaluable and, more generally, synchrotron science offers a wealth of opportunities for fundamental and applied research for hydrothermal processes.

The data we have presented here will be greatly enhanced by the proposed simultaneous (i.e. same spot) XRPD/micro-Raman facility at the Canadian Light Source. Such a set-up has already been developed at several synchrotron facilities [33, 34], and the addition of this technique will be advantageous in developing the HDAC experimental capabilities. In this work, we have primarily employed both Raman spectroscopic measurements and X-ray powder diffraction to determine the crystallinity of relevant moieties. In future work, the complementary nature of these two techniques will be fully employed, i.e., to measure the functional group transformations via Raman spectroscopy and the consequent crystalline sample changes using XRPD.

Our observations suggest potential uses of SCW as a useful medium for solar energy applications, and identify some intriguing features of SCW research. The results of our study also provide the possibility for measurement of in situ

time-resolved profiles of chemical reactions, catalyst stability and residue formation in hydrothermal processing.

REFERENCES

- [1] M. Hodes, P. A. Marrone, G. T. Hong, K. A. Smith and J. W. Tester, *J. Supercritical Fluids*, 2004, 29, 265-288.
- [2] P. A. Marrone, S. D. Cantwell and D. W. Dalton, *Ind. Eng. Chem. Res.*, 2005, 44, 9030-9039.
- [3] M. D. Bermejo and M. J. Cocero, *AIChE J.*, 2006, 52, 3933-3951.
- [4] Z. Fang, T. Minowa, C. Fang, R. L. Smith, H. Inomata and J. A. Kozinski, *International J. Hydrogen Energy*, 2008, 33, 981-990.
- [5] P. E. Bocanegra, C. Reverte, C. Aymonier, A. Loppinet-Serani, M. M. Barsan, I. S. Butler, J. A. Kozinski and I. Gokalp, *J. Supercritical Fluids*, 2010, 53, 72-81.
- [6] C. Calahoo, M. M. Barsan, M. L. Thomas, J. A. Kozinski and I. S. Butler, *Vib. Spectrosc.*, 2011, 57, 2-7.
- [7] A. Sobhy, I. S. Butler and J. A. Kozinski, *Proceedings of the Combustion Institute*, 2007, 31, 3369-3376.
- [8] Z. Fang, H. Assaaoudi, A. Sobhy, M. M. Barsan, I. S. Butler, R. I. L. Guthrie and J. A. Kozinski, *Fuel*, 2008, 87, 353-358.
- [9] A. Sobhy, R. I. L. Guthrie, I. S. Butler and J. A. Kozinski, *Proceedings of the Combustion Institute*, 2009, 32, 3231-3238.
- [10] S. K. Xu, I. Butler, I. Gokalp and J. A. Kozinski, *Proceedings of the Combustion Institute*, 2011, 33, 3185-3194.
- [11] Y. Matsumura, T. Minowa, B. Potic, S.R.A. Kersten, W. Prins, W.P.M van Swaaij, B. van de Beld, D.C. Elliott, G.G. Neuenschwander, A. Kruse and M.J. Antal, *Biomass & Bioenergy*, 2005, 29, 269-292.
- [12] A. Kruse, P. Bernolle, N. Dahmen, E. Dinjus, and P. Maniam, *Energy Environ. Sci.*, 2010, 3, 136-143.
- [13] S. Letellier, F. Marias, P. Cezac and J.P. Serin, *J. Supercritical Fluids*, 2010, 51, 353-361.
- [14] A. Hammerschmidt, N. Boukis, E. Hauer, U. Galla, E. Dinjus, B. Hitzmann, T. Larsen and S.D. Nygaard, *Fuel*, 2011, 90, 555-562.
- [15] W. A. Bassett, A. H. Shen, M. Bucknum and I. M. Chou, *Rev. Sci. Instrum.*, 1993, 64, 2340-2345.
- [16] R. L. Smith and Z. Fang, *J. Supercritical Fluids*, 2009, 47, 431-446.
- [17] K. Syassen, *High Pressure Research*, 2008, 28, 75-126.
- [18] S. Desgreniers and C.-Y. Kim, *Physics in Canada*, 2011, 67, 3-6.
- [19] R. Hashaikeh, Z. Fang, I. S. Butler and J. A. Kozinski, *Proceedings of the Combustion Institute*, 2005, 30, 2231-2237.
- [20] R. Hashaikeh, Z. Fang, I. S. Butler, J. Hawari and J. A. Kozinski, *Fuel*, 2007, 86, 1614-1622.
- [21] Z. Fang and J. A. Kozinski, *Proceedings of the Combustion Institute*, 2000, 28, 2717-2725.
- [22] Z. Fang and J. A. Kozinski, *Combust. Flame*, 2001, 124, 255-267.
- [23] Z. Fang, T. Minowa, R. L. Smith, T. Ogi and J. A. Kozinski, *Ind. Eng. Chem. Res.*, 2004, 43, 2454-2463.
- [24] P. Meerts, *Annals of Forest Science*, 2002, 59, 713-722.
- [25] M. K. Misra, K. W. Ragland and A. J. Baker, *Biomass & Bioenergy*, 1993, 4, 103-116.

- [26] J. W. Hudgins, T. Krekling and V. R. Franceschi, *New Phytologist*, 2003, 159, 677-690.
- [27] J. Xu, D. F. R. Gilson, I. S. Butler and I. Stangel, *J. Biomedical Materials Research*, 1996, 30, 239-244.
- [28] S. P. Parthiban, K. Elayaraja, E. K. Girija, Y. Yokogawa, R. Kesavamoorthy, M. Palanichamy, K. Asokan and S. N. Kalkura, *J. Materials Science: Materials in Medicine*, 2009, 20, S77-S83.
- [29] G. J. Piermarini, S. Block, J. D. Barnett and R. A. Forman, *J. Applied Physics*, 1975, 46, 2774-2780.
- [30] S. Yamaoka, O. Shimomura, O. Fukunaga, *Proceedings of the Japan Academy Series B-Physical and Biological Sciences*, 1980, 56, 103-107.
- [31] Y. P. Yang, H. F. Zheng, *Appl. Spectrosc.*, 2009, 63, 120-123.
- [32] I. M. Chou, *International Geology Review*, 2007, 49, 289-300.
- [33] R. J. Davies, M. Burghammer and C. Riekel, *Applied Physics Letters*, 2005, 87, 264105.
- [34] E. Boccaleri, F. Carniato, G. Croce, D. Viterbo, W. van Beek, H. Emerich and M. Milanesio, *J. Applied Crystallography*, 2007, 40, 684-693.